ELSEVIER

Journal of Alloys and Compounds 255 (1997) 190–194

Journal of ALLOYS AND COMPOUNDS

Crystal structure of $Zn_{3.77}V_{1.54}Mo_{1.46}O_{12}$ containing ZnO_6 trigonal prisms

Xiandong Wang, Kevin R. Heier, Charlotte L. Stern, Kenneth R. Poeppelmeier*

Department of Chemistry, Northwestern University, Evanston IL 60208-3113, USA

Received 16 September 1996

Abstract

Single crystals of $Zn_{3.77}V_{1.54}Mo_{1.46}O_{12}$ were grown in a $ZnO/V_2O_5/MoO_3$ melt. The colorless needles were determined to be orthorhombic, space group $P2_12_12_1$ (No. 19), a=5.048 (4) Å, b=10.400 (2) Å, c=17.560 (7) Å, V=921.9(6) Å^3, and Z=4. One type of zinc cation in the structure exhibits trigonal prismatic coordination, and relatively large distortions of the Zn–O bond lengths in the trigonal prisms reduce the symmetry from *Pnma* (centrosymmetric) to $P2_12_12_1$ (acentric).

Keywords: $Zn_{3.77}V_{1.54}Mo_{1.46}O_{12}$ structure; Trigonal prism and acentric

1. Introduction

Multicomponent vanadates or molybdates which contain isolated VO_4 or MoO_4 tetrahedra have attracted attention for their promising catalytic properties (high selectivity and conversion) in the dehydrogenation of alkanes [1–4]. In the Mg–V–Mo–O system, isolated $(V/Mo)O_4$ tetrahedra are formed not only in wolframite $MgMoO_4$ [5] and spinel-related magnesium orthovanadate $Mg_3V_2O_8$ [6], but also in $Mg_{2.5}VMoO_8$ [7]. The interesting cation deficient structure of $Mg_{2.5}VMoO_8$, and the fact that its catalytic properties are comparable to $Mg_3V_2O_8$, encouraged the exploration of new moly-vanadates. The structure of $Mg_{2.5}VMoO_8$ has been determined by both powder and single crystal X-ray diffraction [7,8], and is similar to that found for $NaCo_{2.31}(MoO_4)_3$ [9] and $Cu_3Fe_4V_6O_{24}$ [10]. Several other copper and metal-substituted copper molybdates [11–15] display similar structures, which may crystallize in either centrosymmetric *Pnma* or noncentrosymmetric $P2_12_12_1$. In the present work, a new noncentrosymmetric compound, $Zn_{3.77}V_{1.54}Mo_{1.46}O_{12}$, is reported. Through detailed structural comparison of $Zn_{3.77}V_{1.54}Mo_{1.46}O_{12}$ with the similar structures mentioned above, the origin of the noncentrosymmetry has been traced to the trigonal prismatic site.

2. Experimental

2.1. Single crystal growth

Crystals of $Zn_{3.77}V_{1.54}Mo_{1.46}O_{12}$ were grown from the composition 66.66 mol% ZnO, 16.67 mol% V_2O_5 and 16.67 mol% MoO_3. About 6 g of the mixed powder was placed in a platinum boat and heated to 920 °C. After holding at 920 °C for 0.5 h, the melt was first cooled to 800 °C at 6 °C h^{-1}, and subsequently to 20 °C at 120 °C h^{-1}. Colorless or light yellow needle single crystals were readily grown. The crystals varied in length from 0.5 mm to 3 mm and were less than 0.2 mm wide. The face perpendicular to the needle axis is the {100} plane, indicating the fastest growing direction is {100}. The other two faces are {010} and {001} respectively. This growth behavior is similar to $Mg_{2.54}V_{1.08}Mo_{0.92}O_8$ [8]. The melting point of polycrystalline $Zn_{3.75}V_{1.5}Mo_{1.5}O_{12}$, as determined by Differential Thermal Analysis (TA Instruments Thermal Analyst 2000), was approximately 873 °C.

2.2. Structure determination

One colorless and transparent $Zn_{3.77}V_{1.54}Mo_{1.46}O_{12}$ crystal with approximate dimensions of 0.48 mm−0.05 mm−0.03 mm was mounted on a glass fiber for single crystal X-ray diffraction. All measurements were made on an Enraf-Nonius CAD4 diffractometer with graphite monochromated Mo-Kα radiation. The crystal system was determined to be orthorhombic. Unit cell parameters and

*Corresponding author.

0925-8388/97/$17.00
PII S0925-8388(96)02812-5

data collection details are listed in Table 1. The intensities of three standard reflections were measured after every 90 min of X-ray exposure time and no loss of intensity was observed. An analytical absorption correction [16] was applied which resulted in transmission factors ranging from 0.46 to 0.71. The data were corrected for Lorentz and polarization effects, and a correction for secondary extinction was applied.

The systematic absences ($h00$, $h\neq 2n$; $0k0$, $k\neq 2n$; $00l$, $l\neq 2n$) uniquely determined the space group to be $P2_12_12_1$ (No. 19). The structure was solved by direct methods [17] and expanded using Fourier techniques [18]. Zinc and oxygen atoms were refined anisotropically and the disordered vanadium and molybdenum atoms were refined isotropically. The populations of V, Mo and Zn(1) atoms were fixed based on the analyzed composition $Zn_{3.77}V_{1.54}Mo_{1.46}O_{12}$. The final cycle of full-matrix least-squares refinement converged with unweighted and weighted agreement factors: $R=4.1\%$ and $R_w=3.8\%$. The coordinates were inverted and the structure re-refined resulting in R values: $R=4.2\%$ and $Rw=3.9\%$. The reported coordinates are those resulting in the lower R values. Atomic positions, occupancies and thermal displacement parameters are presented in Table 2. Selected interatomic distances are given in Table 3. Vanadium and molybdenum atoms were completely disordered, and the zinc cation vacancies were localized on the Zn(1) site. This model has been tested by Hamilton's statistical method [19] (see Table 4). Other models, such as with cation vacancies not on the Zn(1) site (Models I and II) or with significant ordering of V and Mo on the M1, M2 and M3 sites (Models III and IV), can be rejected at the 0.005 level for the reduction in R. However, the existence of partial ordering of V and Mo between the M1 and M3 sites is possible (Models V and VI). Population refinement on the Zn(1) site gave the formula $Zn_{3.80}V_{1.54}Mo_{1.46}O_{12}$ ($R=4.1\%$, $Rw=3.8\%$, Occ.(Zn1)=0.80 and B_{eq}(Zn1)=3.95(7)), which was consistent with the analyzed composition of $Zn_{3.77}V_{1.54}Mo_{1.46}O_{12}$. All calculations were performed using the TEXSAN crystallographic software package from Molecular Structure Corporation [20].

The investigated crystal was dissolved in nitric acid and the chemical composition determined by Inductively Coupled Plasma Atomic Emission Spectrophotometry (ICP-AES, Thermo Jarrell Ash, model Atomscan 25). The density was measured on polycrystalline $Zn_{3.75}V_{1.50}Mo_{1.50}O_{12}$ at room temperature with apparatus described by Chern et al. [21].

Table 1
Crystal data and details of $Zn_{3.77}V_{1.54}Mo_{1.46}O_{12}$ structure determination[a]

Chemical formula	$Zn_{3.77}V_{1.54}Mo_{1.46}O_{12}$
Formula weight	657.00
Crystal system	Orthorhombic
Space group	$P2_12_12_1$(No. 19)
a	5.048(4) Å
b	10.400(2) Å
c	17.560(7) Å
V	921.9(6) Å^3
Z	4
D_x, D_m[b]	4.73 g cm^{-3}, 4.73 g cm^{-3}
μ(Mo Kα)	131.24 cm^{-1}
Approximate crystal dimensions	0.48×0.05×0.03 mm^3
Radiation, wavelength	Mo Kα, 0.71069 Å
Monochromator	Graphite
Temperature	−120.0 °C
Scan type, rate	$\omega-\theta$, 3–15°min^{-1} (in ω)
$2\theta_{max}$	59.9°
No. of reflection measured	total: 2006
	unique: 1606 (R_{int}=0.054)
No. of observations ($I>3.00\sigma(I)$)	1089
No. of variables	158
Residuals	
$R=\Sigma\|\|F_{obs}-F_{calc}\|\|/\Sigma F_{obs}$	0.041
Rw[c]$=[\Sigma w(F_{obs}-F_{calc})^2/\Sigma w F_{obs}^2]^{1/2}$	0.038
Goodness of fit	1.82
Shift/error	0.37
Final difference Fourier peaks (max, min)	2.16, −1.49 e$^-$/Å^3
Flack parameter	−0.012(7)

[a] Further details of the crystal structure determination can be ordered from Fachinformationszentrum Karlsruhe, 76344 Eggenstein-Leopoldshafen, under the depository number CSD-No. 405961.
[b] Measured on $Zn_{3.75}V_{1.50}Mo_{1.50}O_{12}$ powder.
[c] $w=1/\sigma^2(F_{obs})$.

Table 2
Atomic coordinates, occupation factors and equivalent temperature parameters B_{eq}(Å^2) for the $Zn_{3.77}V_{1.54}Mo_{1.46}O_{12}$ structure

Atom	x	y	z	Occ.	B_{eq}[a]
Mo(1)	0.2195(3)	0.7433(2)	0.80632(7)	0.485	0.43(2)[b]
Mo(2)	0.7235(6)	0.0197(1)	0.90191(10)	0.485	0.61(3)[b]
Mo(3)	−0.2796(7)	0.4638(2)	0.9101(1)	0.485	0.98(4)[b]
V(1)	0.2195(3)	0.7433(2)	0.80632(7)	0.515	0.43(2)[b]
V(2)	0.7235(6)	0.0197(1)	0.90191(10)	0.515	0.61(3)[b]
V(3)	−0.2796(7)	0.4638(2)	0.9101(1)	0.515	0.98(4)[b]
Zn(1)	0.3975(7)	0.7514(6)	0.9984(2)	0.77	3.70(7)
Zn(2)	0.2508(4)	0.2418(2)	0.94452(8)	1.0	1.19(3)
Zn(3)	0.2498(10)	0.0697(1)	0.7748(1)	1.0	0.92(4)
Zn(4)	−0.2463(10)	0.9104(1)	0.7184(1)	1.0	0.89(4)
O(1)	0.930(4)	0.117(1)	0.9568(8)	1.0	1.7(3)
O(2)	0.915(3)	0.981(1)	0.8224(7)	1.0	0.7(3)
O(3)	0.442(4)	0.107(1)	0.8735(8)	1.0	0.9(3)
O(4)	0.643(4)	0.881(1)	0.9532(8)	1.0	1.4(3)
O(5)	0.419(3)	0.876(1)	0.7843(8)	1.0	0.8(3)
O(6)	0.140(2)	0.747(1)	0.9013(5)	1.0	1.1(2)
O(7)	0.414(3)	0.609(1)	0.7892(8)	1.0	0.7(2)
O(8)	−0.056(2)	0.741(1)	0.7429(5)	1.0	0.9(2)
O(9)	−0.347(3)	0.604(1)	0.9557(7)	1.0	0.9(3)
O(10)	−0.092(3)	0.496(1)	0.8301(7)	1.0	0.7(2)
O(11)	−0.078(3)	0.366(1)	0.9677(8)	1.0	1.1(3)
O(12)	−0.563(3)	0.375(1)	0.8813(7)	1.0	0.6(2)

[a] $B_{eq}=\frac{8}{3}\pi^2(U_{11}(aa^*)^2+U_{22}(bb^*)^2+U_{33}(cc^*)^2+2U_{12}aa^*bb^*\cos\gamma+2U_{13}aa^*cc^*\cos\beta+2U_{23}bb^*cc^*\cos\alpha)$.
[b] Isotropically refined atoms.

Table 3
Selected interatomic distances (Å) and bond angles (°) in the $Zn_{3.77}V_{1.54}Mo_{1.46}O_{12}$ structure

M(1)–O(6)	1.716(9)	Zn(2)–O(12)	2.01(1)	O(1)–Zn(2)–O(1)	125.9(5)
–O(7)	1.73(1)	–O(1)	2.09(2)	O(1)–Zn(2)–O(3)	90.1(6)
–O(5)	1.75(1)	–O(11)	2.09(1)		130.5(7)
–O(8)	1.781(9)	–O(3)	2.11(1)	O(1)–Zn(2)–O(11)	69.3(4)
M(2)–O(1)	1.74(2)	–O(11)	2.14(2)		75.7(4)
–O(2)	1.74(1)	–O(1)	2.44(1)		77.9(7)
–O(4)	1.75(1)	Zn(3)–O(3)	2.02(2)		84.9(7)
–O(3)	1.76(2)	–O(8)	2.06(1)	O(1)–Zn(2)–O(12)	78.7(5)
M(3)–O(9)	1.70(1)	–O(7)	2.08(2)		148.1(6)
–O(10)	1.73(1)	–O(2)	2.10(1)	O(3)–Zn(2)–O(11)	83.6(6)
–O(11)	1.76(1)	–O(10)	2.15(1)		150.1(6)
–O(12)	1.78(1)	–O(5)	2.19(1)	O(3)–Zn(2)–O(12)	85.4(3)
Zn(1)–O(4)	2.00(2)	Zn(4)–O(12)	2.03(1)	O(11)–Zn(2)–O(11)	120.2(4)
–O(4)	2.06(2)	–O(8)	2.05(1)	O(11)–Zn(2)–O(12)	92.9(5)
–O(9)	2.11(1)	–O(5)	2.08(2)		125.8(6)
–O(6)	2.14(1)	–O(10)	2.10(2)		
–O(9)	2.14(2)	–O(2)	2.13(1)		

3. Results and discussion

3.1. Structure description

In the $Zn_{3.77}V_{1.54}Mo_{1.46}O_{12}$ structure (Fig. 1), $Zn(3)O_6$ and $Zn(4)O_6$ octahedra form the zigzag sheets by sharing edges and corners, face-sharing $Zn(1)O_6$ octahedra form one-dimensional chains passing through the center of hexagonal tunnels, and the very unusual $Zn(2)O_6$ trigonal prisms form columns parallel to the *a* axis. Disordered $(V/Mo)O_4$ tetrahedra are linked to ZnO_6 octahedra and/or trigonal prisms by sharing corners to form the three dimensional framework. The mutual linkage among different polyhedra are identical to that described in $Mg_{2.54}V_{1.08}Mo_{0.92}O_8$ [8].

The Zn–O bond lengths of 2.00–2.23 Å (Table 3) for the three ZnO_6 octahedra are fairly normal compared to other zinc oxides (e.g. α-$ZnMoO_4$ and α-$Zn_3V_2O_8$ [22,23]). Similarly, (V/Mo)–O bond lengths for MO_4 tetrahedra (1.70–1.78 Å) compare well with (V/Mo)–O bond lengths in $Mg_{2.54}V_{1.08}Mo_{0.92}O_8$ (1.71–1.77 Å) [8] and in $Mn_{2.47}V_{0.94}Mo_{1.06}O_8$ (1.72–1.78 Å) [24]. Bond valence calculations [25] for the (V/Mo) positions (M1–M3) result in M1=+5.41, M2=+5.35 and M3=+5.44, as compared to Mo=+6.08 (average) in $Cu_{3.85}Mo_3O_{12}$ [11] and V=+4.95 (average) in $Cu_3Fe_4V_6O_{24}$ [10]. Thus, it is

Table 4
Hamilton's test for the disorder of vanadium and molybdenum and the localization of cation vacancies in $Zn_{3.77}V_{1.54}Mo_{1.46}O_{12}$ for the given 158 parameters and 1089 reflections

Model	M configuration and Zn^{2+} cation vacancy[b]	*R*	*Rw*	Shift/error	GFI[a]	*Rw*/0.038 ($\mathcal{R}$)[c]
I	M(0.485Mo+0.515V)[b] Zn(2) (Occ.=0.77)	0.0625	0.0673	5.3	3.2	1.77
II	M(0.485Mo+0.515V)[b] Zn(3) and Zn(4) (Occ.=0.885)	0.0574	0.0689	3.3	3.3	1.81
III	M1(0.4Mo+0.60V) M2(0.57Mo+0.43V) M3(0.485Mo+0.515V) Zn(1) (Occ.=0.77)	0.0435	0.0424	0.7	2.0	1.12
IV	M1(0.64Mo+0.36V) M2(0.485Mo+0.515V) M3(0.33Mo+0.67V) Zn(1) (Occ.=0.77)	0.0436	0.0429	0.29	2.03	1.13
V	M1(0.57Mo+0.43V) M2(0.485Mo+0.515V) M3(0.40Mo+0.60V) Zn(1) (Occ.=0.77)	0.0410 (B_{iso}(M1)=0.69(2), B_{iso}(M2)=0.59(3), B_{iso}(M1)=0.70(3))	0.0385	0.80	1.82	1.01
VI	M1(0.53Mo+0.47V) M2(0.485Mo+0.515) M3(0.44Mo+0.56V) Zn(1) (Occ.=0.77)	0.0407 (B_{iso}(M1)=0.57(2), B_{iso}(M2)=0.60(3), B_{iso}(M3)=0.83(3))	0.0377	0.19	1.78	0.99

[a] GFI: Goodness of fit indicator.
[b] M=M1, M2 and M3.
[c] Interpolation from the Table in [18] gives $\mathcal{R}_{158,\,931,\,0.005}=1.109$.

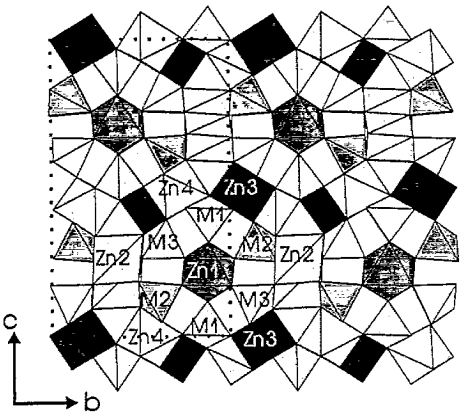

Fig. 1. Structure of $Zn_{3.77}V_{1.54}Mol_{1.46}O_{12}$ (two unit cells) viewed along the *a* axis. Metal–oxygen polyhedra are labeled. M1, M2 and M3 stand for disordered vanadium and molybdenum (V/Mo).

unlikely that any obvious vanadium and molybdenum ordering occurs among the three tetrahedral sites. However, some ordering is still possible between V and Mo on the M1 and M3 sites (Table 4). The fairly large differences in the thermal parameters among the V/Mo positions can be reduced by making the M1 site slightly Mo rich, and the M3 site slightly V rich (see Table 2 and Table 4). Quantitative determination of such partial ordering of V and Mo, if it exists, may require the use of neutron diffraction.

The zinc cation deficiency occurs at the face-sharing octahedral positions, which is equivalent to the magnesium deficiency in $Mg_{2.54}V_{1.08}Mo_{0.92}O_8$. The occupancy of Zn(1) is slightly smaller than Mg^{2+} in $Mg_{2.54}V_{1.08}Mo_{0.92}O_8$ (Table 5), and both are appreciably larger than the copper occupancy in $Cu_3Fe_4V_6O_{24}$. The unusual face-sharing $Zn(1)O_6$ octahedra give rise to Zn^{2+}–Zn^{2+} distances of 2.53 Å, even shorter than the Zn–Zn distances (2.67 Å) in zinc metal [26]. A relatively large thermal displacement for Zn(1) was found with the thermal ellipsoids elongated in the direction of the hexagonal tunnel and inclined along the *b* direction (Fig. 2). The shape of the thermal ellipsoid is attributed to the displacements of the zinc cations resulting from coulombic repulsions between $Zn(1)^{2+}$ ions. The high B_{eq} values 1.4–1.7 $Å^2$ (see Table 2) for the oxygen positions are slightly larger than those (i.e. 1.0–1.1 $Å^2$) in $Mg_{2.54}V_{1.08}Mo_{0.92}O_8$ [8].

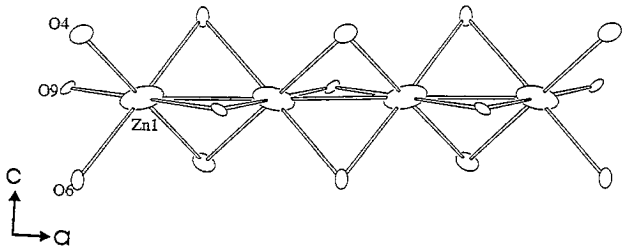

Fig. 2. Thermal ellipsoids (50%) for the $Zn(1)O_6$ face-shared octahedra.

3.2. Trigonal prismatic ZnO_6

Nothing is unusual in the framework of ZnO_6 octahedra and $(V/Mo)O_4$ tetrahedra compared with their counterparts in the centrosymmetric $Mg_{2.54}V_{1.08}Mo_{0.92}O_8$, therefore the symmetry reduction ($Pnma \rightarrow P2_12_12_1$) is most likely due to distortions in the very unusual trigonal prismatic $Zn(2)O_6$ site. $Zn(2)O_6$ is a distorted trigonal prism (Fig. 3(a)), with one Zn(2)–O(1) bond (2.44 Å) which is longer than any other Zn–O bond (2.0–2.2 Å) in the structure (Table 3). One short Zn(2)–O(1) bond (2.09 Å) and one long Zn(2)–O(1) bond (2.44 Å) are bridged to the long and short Zn(2)–O(1) bonds, respectively, of adjacent $Zn(2)O_6$ trigonal prisms (Fig. 3b). This alternating short–long Zn(2)–O(1) connection reduces the *a* glide plane in *Pnma* to a 2_1 screw axis parallel to the *a* axis. O(1) is further bonded to the M2 position so that the symmetry reduction is extended, making M2 and M3 inequivalent. The origin of the $Zn(2)O_6$ distortion is unclear. Ion size effects ($r(Mg^{2+}) < r(Zn^{2+}) < r(Mn^{2+})$ [27]) do not alone explain the reduction in symmetry, whereas a rigid coordination model could explain the rare observation of trigonal prismatic coordination, as was also recently reported in Sr_3ZnPtO_6 [28].

Table 5
Space groups, cation occupancy of the face-shared octahedra (F.S.O), *d* electron count (d^n) for the cations adopting non-octahedral coordination (N.O.C.) in some oxides with similar framework structures as $Zn_{3.77}V_{1.54}Mo_{1.06}O_8$

Oxides	S.G.	F.S.O.	Occ.	N.O.C.	d^n	Ref.
$NaCo_{2.31}(MoO_4)_3$	*Pnma*	$Co^{2+/3+}O_6$	0.75	Na^+O_6 TP	0	[9]
$Mg_{2.54}V_{1.08}Mo_{0.92}O_8$	*Pnma*	MgO_6	0.81	$Mg^{2+}O_6$ TP	0	[8]
$Mn_{2.47}V_{0.94}Mo_{1.06}O_8$	*Pnma*	MnO_6	0.705	$Mn^{2+}O_6$ TP	5	[24]
$(Cu,Mn)_{3.66}Mo_3O_{12}$	*Pnma*	$(Cu,Mn)O_6$	0.66	$(Cu^+,Mn^{2+})O_6$ TP	–	[15]
$(Cu,Co)_{3.75}Mo_3O_{12}$	*Pnma*	$(Cu,Co)O_6$	0.75	$(Cu,Co)O_6$ TP	–	[13]
$Cu_3Fe_4V_6O_{24}$	*Pnma*	CuO_6	0.50	$Cu^{2+}O_4$ SP	9	[10]
$(Cu,Fe)_{3.63}Mo_3O_{12}$	$P2_12_12_1$	$(Cu,Fe)O_6$	0.63	$(Cu,Fe)O_6$ SPy	–	[14]
$Cu_{3.85}Mo_3O_{12}$	$P2_12_12_1$	CuO_6	0.85	CuO_6 SPy	–	[11]
$(Cu,Zn)_{3.75}Mo_3O_{12}$	$P2_12_12_1$	$(Cu,Zn)O_6$	0.75	Cu^+O_6 SPy	10	[12]
$Zn_{3.77}V_{1.54}Mo_{1.46}O_{12}$	$P2_12_12_1$	ZnO_6	0.77	$Zn^{2+}O_6$ DTP	10	this work

TP: trigonal prism, SP: square planar, SPy: square pyramid, DTP: distorted trigonal prism.

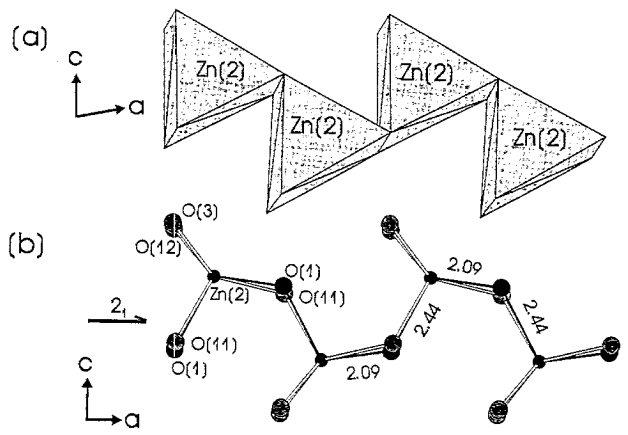

Fig. 3. (a) Distorted $Zn(2)O_6$ trigonal prisms; (b) String of $Zn(2)O_6$ viewed along the *b* axis showing the coordination of Zn(2), the alternating short–long Zn(2)–O(1) bonds (O(1), (solid black) and the 2-fold screw axis.

The three other known acentric compounds with structures similar to $Zn_{3.77}V_{1.54}Mo_{1.46}O_{12}$ all contain distorted square pyramids, which can also be viewed as strongly distorted trigonal prisms (see Table 5). In $Cu_{3.85}Mo_3O_{12}$ five Cu–O bonds in such CuO_6 'trigonal prisms' fall within 2.03–2.28 Å but the sixth bond reaches 2.81 Å. Similar coordination environments are found in $(Cu, Zn)_{3.75}Mo_3O_{12}$ and $(Cu, Fe)_{3.63}Mo_3O_{12}$. By contrast, the centrosymmetric compounds with this structure contain regular trigonal prismatic coordination with either three pairs of similar metal–oxygen bond lengths ($NaCo_{2.31}(MoO_4)_3$, $Mg_{2.54}V_{1.08}Mo_{0.92}O_8$ and $Mn_{2.47}V_{0.94}Mo_{1.06}O_8$), or with one pair longer than the other two ($(Cu, Mn)_{3.66}Mo_3O_{12}$ and $(Cu, Co)_{3.75}Mo_3O_{12}$). There is also one example of square planar coordination owing to the Jahn-Teller effect ($Cu_3Fe_4V_6O_{24}$). Thus, the decrease in symmetry from *Pnma* to $P2_12_12_1$ is largely reflected in a distortion of the trigonal prismatic groups rather than changes in the octahedral or tetrahedral groups.

4. Conclusions

The crystal structure of $Zn_{3.77}V_{1.54}Mo_{1.46}O_{12}$ was determined to be similar to the moly-vanadate $Mg_{2.54}V_{1.08}Mo_{0.92}O_8$, the vanadate $Cu_3Fe_4V_6O_{24}$ and several molybdates such as $NaCo_{2.31}(MoO_4)_3$ and $Cu_{3.85}Mo_3O_{12}$. The reduction in symmetry from *Pnma* to $P2_12_12_1$ has been discussed in terms of the distortion of the unusual trigonal prismatic $Zn(2)O_6$ groups. Although $Zn_{3.77}V_{1.54}Mo_{1.46}O_{12}$ is not polar, ruling out pyroelectric or ferroelectric behavior, a second-order non-linear-optical (NLO) response is still possible. Measurements are in progress to determine the magnitude of the NLO signal.

Acknowledgments

The authors wish to thank Dr. Larry Cirjak and acknowledge an Extramural Research Award (EMRA) from BP America, the National Science Foundation (NSF) (No. DMR-9412971) and the MRC of Northwestern University supported by NSF (No. DMR-9120521) for support of this research work.

References

[1] G.A. Stepanov, A.L. Tsailinggol'd, V.A. Levin and F.S. Pilipenko, *Stud. Surf. Sci. Catal., B7* (1981) 1293.
[2] M.A. Chaar, D. Patel, M.C. Kung and H.H. Kung, *J. Catal., 105* (1987) 483.
[3] W.D. Harding, H.H. Kung, V.L. Kozhevnikov and K.R. Poeppelmeier, *J. Catal., 144* (1993) 597.
[4] O.S. Owen and H.H. Kung, *J. Mol. Catal., 79* (1993) 265.
[5] V.V. Bakakin, R.F. Klevtsova and L.A. Gaponenko, *Kristallografiya, 27* (1982) 38.
[6] N. Krishnamachari and C. Calvo, *Canad. J. Chem., 49* (1971) 1629.
[7] V.G. Zubkov, I.A. Leonidov, K.R. Poeppelmeier and V.L. Kozhevnikov, *J. Solid State Chem., 111* (1994) 197.
[8] X.D. Wang, C.L. Stern and K.R. Poeppelmeier, *J. Alloy and Compound.*, in press.
[9] J.A. Ibers and G.W. Smith, *Acta Cryst., 17* (1964) 190.
[10] J.M. Hughes, S.J. Starkey, M.L. Malinconico and L.L. Maliconico, *Amer. Mineral., 72* (1987) 1000.
[11] L. Katz, A. Kasenally and L. Kihlborg, *Acta Crystallog., B27* (1971) 2071.
[12] Szillat, Hk. Müller-Buschbaum, *Z. Naturforsch., 50B* (1995) 247.
[13] Szillat, Hk. Müller-Buschbaum, *Z. Naturforsch., 50B* (1995) 707.
[14] O. Sedello and Hk. Müller-Buschbaum, *Z. Naturforsch., 51B* (1996) 90.
[15] O. Sedello, Hk. Müller-Buschbaum, *Z. Naturforsch., 51B* (1996) 447.
[16] J. de Meulenaer and H. Tompa, *Acta Cryst., 19* (1965) 1014.
[17] G.M. Sheldrick, SHELX86, in G.M. Sheldrick, C. Kruger and R. Goddard (eds), *Crystallographic Computing 3*, Oxford University Press, 1985, p. 175.
[18] P.T. Beurskens, G. Admiraal, G. Beurskens, W.P. Bosman, S. Garcia-Granda, R.O. Gould, J.M.M. Smits and C. Smykalla, DIRDIF92, in The DIRDIF program system, Technical Report of the Crystallography Laboratory, University of Nijmegen, The Netherlands, 1992.
[19] W.C. Hamilton, *Acta Cryst., 18* (1965) 505.
[20] TEXSAN-TEXRAY Structure Analysis Package Molecular Structure Corporation, 1985.
[21] M.Y. Chern, R.D. Mariani, D.A. Vennos and F.J. DiSalvo, *Rev. Sci. Instrum., 61* (1990) 1733.
[22] S.C. Abrahams, *J. Chem. Phys., 46* (1967) 2052; *Revue de Chimie Minerale, 20* (1983) 88.
[23] R. Gopal and C. Calvo, *Canad. J. Chem., 49* (1971) 3056.
[24] X.D. Wang, K. Heier, C.L. Stern and K.R. Poeppelmeier, in preparation.
[25] I.D. Brown and D. Altermatt, *Acta Cryst., B41* (1985) 244.
[26] D.R. Lide (ed), in *Handbook of Chemistry and Physics* (72nd), 9–1, CRC Press, 1991–1992.
[27] R.D. Shannon, *Acta Crystallogr., A32* (1976) 751.
[28] C. Lampe-Onnerud and H.C. Loye, *Inorg. Chem., 35* (1996) 2155.